Linearized impulse wave propagating down a vertical column of heavy particles

E. Hascoët[1] and E. J. Hinch[2]
[1]*Fachbereich Physik, Philipps Universität Marburg, D-35032 Marburg, Germany*
[2]*Department of Applied Mathematics and Theoretical Physics, University of Cambridge, Silver Street, Cambridge CB3 9EW, United Kingdom*

(Received 7 January 2002; published 25 July 2002)

A granular column is subjected to a small amplitude impact on its top. For a generalized power-law contact force between neighboring grains, numerical simulations show that the propagation of the impulse wave is controlled by dispersion. This leads quantitatively to a power-law decrease of the amplitude of the wave with depth. We find numerically the dependence of this power-law exponent on the force-law exponent. An analytic expression for the decrease is then derived from a long-wave approximation.

DOI: 10.1103/PhysRevE.66.011307 PACS number(s): 45.70.−n, 43.25.+y, 46.40.−f

I. INTRODUCTION

The propagation of an impulse wave along a horizontal elastic granular chain has received growing attention. First, Nesterenko [1,2] provided a long-wavelength theory for a generalized contact force between the grains, $F \propto \delta^{\alpha}$, where δ is the overlap, i.e., the approach of the centers of the particles in excess of the undeformed contact. This theory has been compared with experiments by Lazaridi and Nesterenko [3] and more recently by Coste, Falcon, and Fauve [4]. Numerical simulations have been performed by Hinch and Saint-Jean [5] and Hascoët and Hermann [6] showing agreement with Nesterenko's theory when the force-law exponent α is close to unity, the Hertzian case $\alpha=\frac{3}{2}$ indicating some discrepancies. Improvements of Nesterenko's theory for the shape of the solitary waves have been given by Chatterjee [7]. The scattering of traveling solitary waves by an impurity mass has also been investigated [6]. The problem of a linear contact force in compression $\alpha=1$ has been studied numerically [5,8] and a long-wavelength theory provided [5].

Waves in vertical granular columns, implying effects of gravity, were first studied by Sinkovits and Sen [9,10], who considered the propagating signal due to a weak perturbation at the top surface of a granular column. It was then checked numerically that the phase velocity of the traveling signal varies with $z^{1/2(1-1/\alpha)}$, where z is the depth in the column. A numerical study of the scattering of the propagating signal by an impurity has also been provided [11] and the detection of buried objects was then proposed as an application. The dispersive nature of the propagating waves in the linear regime has been investigated more precisely by Hong, Ji, and Kim [12]. A theory for the observed power laws for the decrease of the amplitudes of the displacement and velocity was then proposed.

In this paper, we propose an alternative derivation of these power laws consistent with the dispersive nature of wave propagation in the granular column. The dispersive feature of propagation was not taken into account in the previous work [12] since the partial differential equation for the grain displacement obtained at the continuum limit does not contain dispersive terms leading to inconsistencies in the derivation of the power laws. Our theory is based on a long-wavelength approximation that enables one to go further in the spatial derivatives of the displacement, leading to additional fourth-order derivatives modeling dispersion in the partial differential equation. It is worth saying that this procedure is the same as the one used for introducing dispersion in the case of the horizontal granular chain (see [1,2,5]). We then extract an approximation for the exponent of the observed power laws from the partial differential equation by analytically investigating the evolution of the phase of the wave in the slowly varying medium.

II. EQUATIONS OF MOTION

We consider a column of N particles of mass m with a particle interaction force $F=k\delta^{\alpha}$, where k is an elastic constant, δ the overlap between two balls, and $\alpha>1$ an exponent determining the kind of contacts between the balls. For instance, $\alpha=1$ for flat planar surfaces, $\alpha=\frac{3}{2}$ for the Hertzian interaction between spherical balls, whereas $\alpha=2$ defines an interaction with conical asperities. We write the contact force between the balls n and $n+1$ as

$$F_{n+1/2}=k(w_n-w_{n+1})_+^{\alpha}.$$

The variable w_n corresponds to the displacement of the ball n from its gravity-free equilibrium position. The label plus on the right bracket means that the force is zero when the balls do not touch, that is $F_{n+1/2}=0$ if $w_n-w_{n+1}<0$.

The equation of motion for the displacement of the grain number n, $1<n<N$ and n increasing with depth, is the following:

$$m\ddot{w}_n=F_{n-1/2}-F_{n+1/2}+mg. \tag{1}$$

The boundary conditions are chosen such that the surface is free and the bottom fixed, hence $F_{1/2}=0$ and $w_N=0$. At time $t=0$, all the particles are at rest in their equilibrium position under gravity and then the first particle is given a velocity V.

The equilibrium values $\overline{w}_n$ are determined by the equilibrium condition when the column is at rest:

$$\overline{F}_{n-1/2}-\overline{F}_{n+1/2}+mg=0.$$

Summing from the beginning of the chain $n=1$ gives

$$\overline{F}_{n+1/2}=mgn.$$

Or, equivalently

$$\overline{w}_n-\overline{w}_{n+1}=\left(\frac{mg}{k}n\right)^{1/\alpha}.$$

Since we focus on small amplitude perturbations about the equilibrium state, the displacement relative to the equilibrium $w'_n=w_n-\overline{w}_n$ must satisfy

$$w'_n-w'_{n+1}\ll\left(\frac{mg}{k}n\right)^{1/\alpha}. \tag{2}$$

This allows us to linearize the equations of motion about the basic state. If we develop $F_{n+1/2}$ to first order in a Taylor expansion we have

$$F_{n+1/2}=\overline{F}_{n+1/2}+\alpha k\left(\frac{mg}{k}\right)^{(\alpha-1)/\alpha}n^{(\alpha-1)/\alpha}(w'_n-w'_{n+1}).$$

Substituting this expression into Eq. (1) we obtain the linearized equations of motion. In order to work with nondimensional quantities we define the velocity scale by V, the impact velocity of the first particle. The corresponding time scale is given by the rescaled equation of motion for this particle. A simple calculation gives us for the time scale T:

$$\frac{m}{T^2}=\alpha k\left(\frac{mg}{k}\right)^{(\alpha-1)/\alpha}.$$

In terms of the velocity scale V and the time scale T, the linearity condition (2) becomes

$$VT\ll\left(\frac{mg}{k}\right)^{1/\alpha}.$$

The nondimensional linearized equations are then

$$\ddot{w}'_n=(n-1)^{(\alpha-1)/\alpha}(w'_{n-1}-w'_n)-n^{(\alpha-1)/\alpha}(w'_n-w'_{n+1}) \tag{3}$$

with $w'_n(0)=0$ and $\dot{w}'_1(0)=1$, $\dot{w}'_n(0)=0$ for $n>1$.

III. NUMERICAL RESULTS

The equations of motion (3) have been integrated numerically using a Gear predictor-corrector algorithm of order five. We first simulated a column with $N=10^3$ particles obeying the Hertzian interaction law. Figure 1 displays the displacement fields at four equal time intervals. A perturbation with speed increasing with depth, and amplitude decreasing, travels down the column. This perturbation is followed by small oscillations with increasing apparent wavelength. The corresponding velocity profiles are displayed in Fig. 2. The velocity perturbation shares the same property of decreasing amplitude. Both amplitudes seem to decrease with depth with a power-law dependence. In order to quantify these decreases, we measured the waves' amplitudes in taller columns of $N=10^4$ particles. In addition, the exponent of the interaction force was varied in a range from 1.5 to 5. The simulations provided two power laws for the decay of the amplitudes: $w_{max}(z)\propto z^{-\beta_1}$ and $v_{max}(z)\propto z^{-\beta_2}$, where z is the position of the maximum amplitude in the column. Due to the discrete nature of the system, those maximum amplitudes oscillate as they decay, as the maximum of the wave travels from one particle to the next. In order to obtain a better approximation of a maximum amplitude and its location, we first looked down the column for the particle with the maximum value of displacement or velocity at a given time. We then measured the corresponding values for the two neighboring particles and made a quadratic interpolation to give a local expression for the variation of the amplitudes between the particles. The maximum amplitude was then extracted by maximizing the quadratic. The values of the exponents β_1 and β_2 were then found first by computing

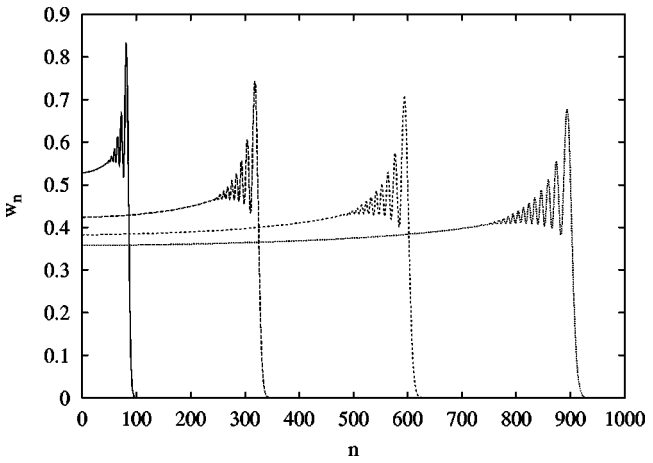

FIG. 1. Displacements of the grains in the column at times $t=50.0$, 150.0, 250.0, and 350.0, and for the case $\alpha=\frac{3}{2}$.

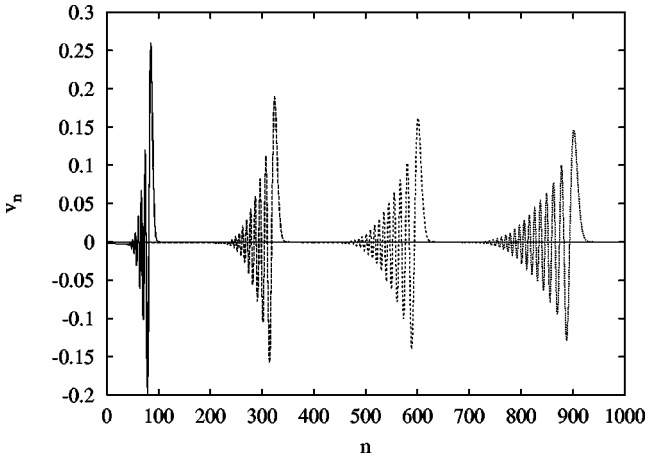

FIG. 2. Velocities of the grains at the same times as for the displacements in Fig. 1.

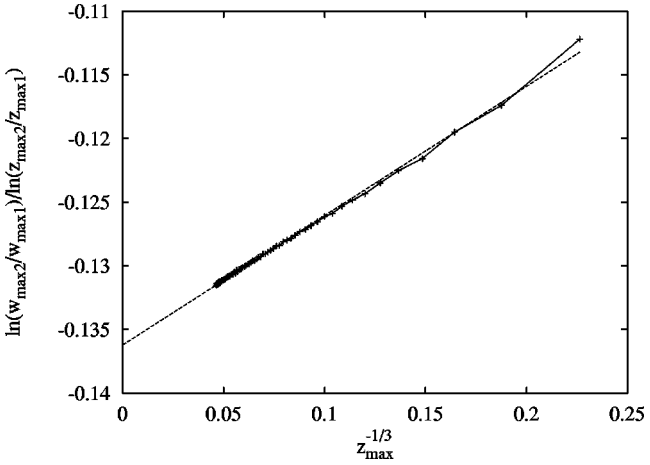

FIG. 3. Determination of the exponent β_1 in the case $\alpha=2$. The local exponent $\ln(w_{max2}/w_{max1})/\ln(z_{max2}/z_{max1})$ is computed until the pulse reaches the position $n=10^4$. w_{max2} and w_{max1} are two displacement maxima measured with a time interval of 10. The asymptotic value of the exponent is extracted at the crossing of the extrapolated line with the vertical axis.

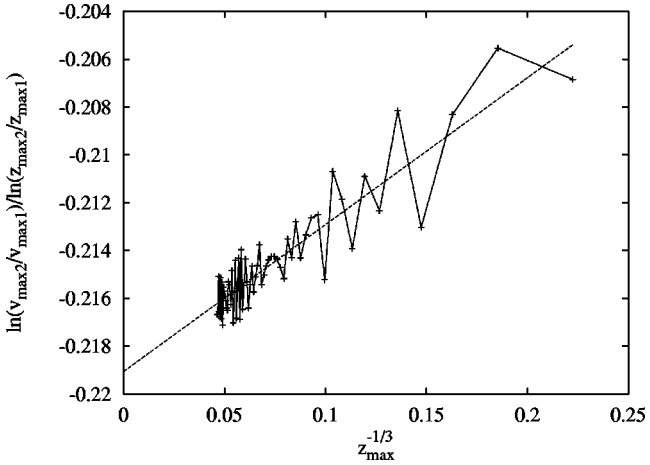

FIG. 4. Determination of the exponent β_2 in the case $\alpha=2$. The same method is used as for β_1. The value obtained is less accurate for the velocity due to the oscillations coming from kinetic and potential energy redistribution in the pulse.

the logarithm of the ratio of two maxima measured at a time interval of ten units divided by the logarithm of the ratio of the corresponding positions. This expression is an estimation of the local decay exponent. These local exponents were then plotted against the inverse of the cube root of the position. The advantage of such a procedure comes from the fact that the local exponents vary linearly with this argument for large enough depth. The reasons for this linear dependence will become clear in the following section where a theory for the impulse propagation is proposed. Figures 3 and 4 give an example of this finite-size extrapolation procedure for $\alpha=2.0$. In the following table we give the values we measured for β_1 and β_2 to an accuracy of three digits.

α	β_1	β_2
1.5	0.101	0.268
2.0	0.136	0.219
3.0	0.167	0.189
4.0	0.187	0.194
5.0	0.200	0.202

The decay exponent β_2 is always larger than β_1, i.e., the velocity decays more rapidly with depth than the displacement. For $\alpha<3$, β_1 increases with α whereas β_2 decreases. As $\alpha>3$, one can notice that β_2 begins to increase. The aim of the following section will be to find functional expressions for β_1 and β_2 justifying these numerical results.

IV. SLOWLY VARYING LONG WAVES

The numerical solutions of the propagating impulse wave show that the wave spreads out slowly. We thus seek to make a long-wave approximation to Eq. (3). We move from a discrete description of the displacements of the individual particles $w_n(t)$ to a continuum representation $w(z,t)$, identifying the discrete n with the continuous z by $z=n$, and for greater clarity we drop the primes in Eq. (3). Let the nondimensional spring constant be

$$K(z)=z^{(\alpha-1)/\alpha}. \tag{4}$$

Then by making a Taylor series expansion of the finite differences in Eq. (3) and retaining just the first two terms, we obtain the governing equation for the continuum long-wave approximation,

$$\frac{\partial^2 w}{\partial t^2}=\left(\frac{\partial}{\partial z}+\frac{1}{24}\frac{\partial^3}{\partial z^3}\right)K\left(\frac{\partial}{\partial z}+\frac{1}{24}\frac{\partial^3}{\partial z^3}\right)w. \tag{5}$$

Thus locally the waves satisfy a dispersion relation,

$$\omega=\Omega(k;z)=\pm K^{1/2}(z)k\left(1-\frac{1}{24}k^2\right),$$

with local frequency ω and local wave number k.

We now consider the evolution of a wave-packet propagation according to this dispersion relation through the slowly varying medium. The wave will propagate at the group velocity

$$\dot{z}=c_g=\frac{\partial\Omega}{\partial k}=K^{1/2}\left(1-\frac{1}{8}k^2\right). \tag{6}$$

As it propagates, its local frequency ω and local wave number k change with the corresponding slow changes in the medium,

$$\dot{\omega}=\frac{\partial\Omega}{\partial t}=0, \tag{7}$$

$$\dot{k}=-\frac{\partial\Omega}{\partial z}=-[K^{1/2}(z)]'k\left(1-\frac{1}{24}k^2\right). \tag{8}$$

At the same time the phase θ of the wave packet evolves according to

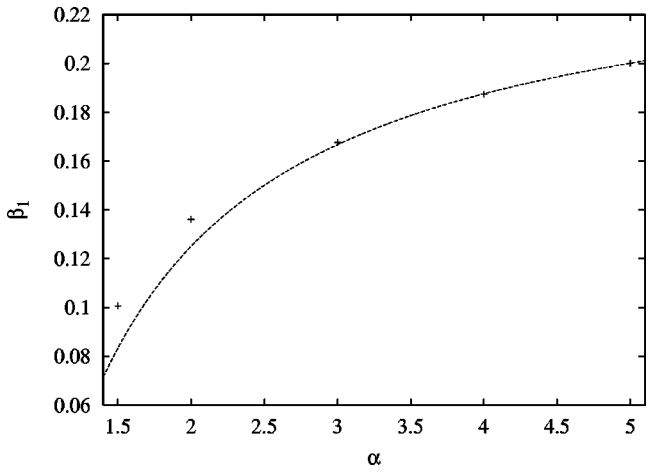

FIG. 5. Numerical and analytic results for the displacement exponent β_1. The analytic result $\beta_1=(\alpha-1)/4\alpha$ corresponds to the dashed curve whereas the numerical results are represented by crosses.

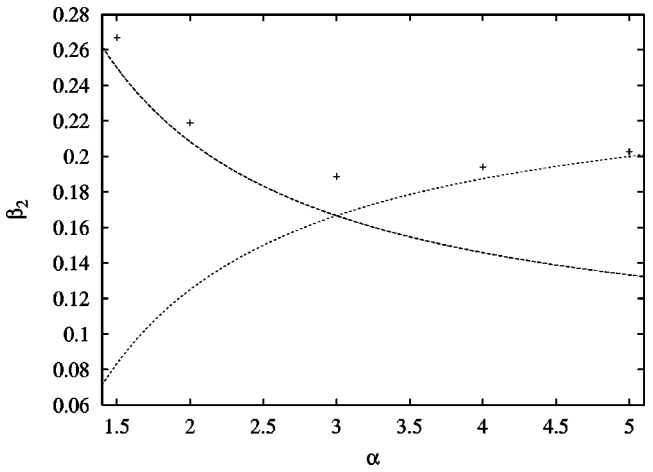

FIG. 6. Numerical and analytic results for the velocity exponent β_2. The analytic results $\beta_2=(\alpha+3)/12\alpha$ if $1<\alpha<3$ and $\beta_2=(\alpha-1)/4\alpha$ if $\alpha>3$ correspond to the two dashed curves whereas the numerical results are represented by crosses.

$$\dot{\theta}=-\Omega+k\frac{\partial\Omega}{\partial k}=-\frac{1}{12}K^{1/2}k^3.$$

Since Eq. (5) describes a Lagrangian system, the amplitude of the wave packet will change conserving wave action $A=E/\omega$, with local energy density E, i.e.,

$$\frac{\partial A}{\partial t}+\frac{\partial}{\partial z}(c_g A)=0. \tag{9}$$

Because the medium does not change in time, the local frequency of a wave packet ω will remain constant. With ω constant, the dispersion gives the variation of the local wave number k as

$$k\left(1-\frac{1}{24}k^2\right)=\omega/K^{1/2}(z).$$

This is in effect the integral of Eq. (8) for the change in the local wave number. As the wave packet propagates down the chain, K increases with z and so k must decrease to zero. Thus we become interested in long waves with small local wave number,

$$k(t)\sim\omega/K^{1/2}(z). \tag{10}$$

We start by tracking the wave packet with zero wave number, $k=0$, as it propagates with its group velocity (6), i.e.,

$$\dot{z}_0=K^{1/2}(z_0)=z_0^{(\alpha-1)/2\alpha},$$

with solution

$$z_0(t)=\left(\frac{\alpha+1}{2\alpha}t\right)^{2\alpha/(\alpha+1)}. \tag{11}$$

This wave packet has a constant phase θ_0.

Now consider a nearby wave packet with a small local frequency ω, which is constant. Let it be at

$$z(\omega,t)=z_0(t)+\Delta z(\omega,t) \quad \text{with} \quad |\Delta z|\ll z_0.$$

This wave packet propagates according to Eq. (6), i.e.,

$$\dot{\Delta z}=\frac{d}{dz}K^{1/2}(z)\big|_{z_0(t)}\Delta z-\frac{1}{8}K^{1/2}(z_0)k^2.$$

Substituting the expression for $K(z)$ in Eq. (4), and our results for $z_0(t)$ in Eq. (11) and for $k(t)$ in Eq. (10), this becomes

$$\dot{\Delta z}=\frac{\alpha-1}{\alpha+1}\frac{\Delta z}{t}-\frac{1}{8}\omega^2\left(\frac{2\alpha}{\alpha+1}\right)^{(\alpha-1)/(\alpha+1)}t^{-(\alpha-1)/(\alpha+1)}.$$

The nature of the solution of this equation at long times depends on the value of the force-law exponent α. For $1<\alpha<3$, the slower group velocity for small nonzero k is important, and

$$\Delta z\to-\frac{1}{8}\omega^2\left(\frac{2\alpha}{\alpha+1}\right)^{(\alpha-1)/(\alpha+1)}\frac{\alpha+1}{3-\alpha}t^{2/(\alpha+1)}. \tag{12}$$

For larger values of the exponent, $\alpha>3$, the local wave number decreases so fast that the wave travels at the same speed as the $k=0$ wave and its different position Δz just represents the accumulation of time delays from early times,

$$\Delta z\to-c_1\omega^2 t^{(\alpha-1)/(\alpha+1)}, \tag{13}$$

where the constant $c_1(\alpha)$ comes from the early time delays.

The evolution of the phase of the wave packets is governed at small frequency by

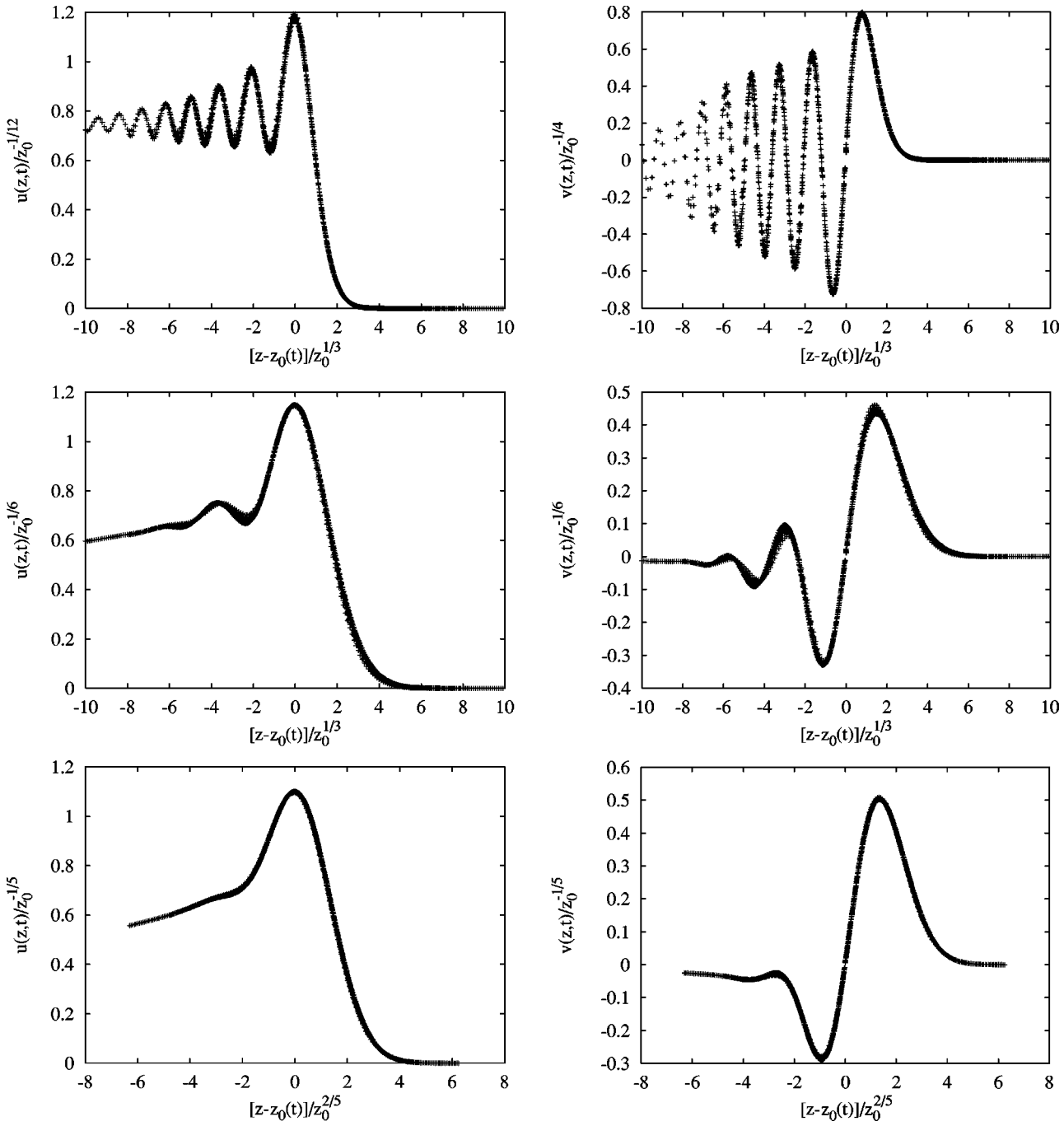

FIG. 7. Wave shapes for displacement and velocity. From top to bottom α is equal to 1.5, 3.0, and 5.0. The displacement pulses are displayed on the left whereas the velocity pulses are displayed on the right.

$$\dot{\theta} = -\frac{1}{12}\frac{\omega^3}{K(z_0(t))} = -\frac{1}{12}\omega^3\left(\frac{2\alpha}{\alpha+1}\right)^{2(\alpha-1)/(\alpha+1)} t^{-2(\alpha-1)/(\alpha+1)}.$$

Again the nature of the solution depends on the value of the exponent α in the force law. For $1<\alpha<3$,

$$\theta = \theta_0 - \frac{1}{12}\omega^3\left(\frac{2\alpha}{\alpha+1}\right)^{2(\alpha-1)/(\alpha+1)}\frac{\alpha+1}{3-\alpha}t^{(3-\alpha)/(\alpha+1)}, \tag{14}$$

while for $\alpha>3$ the wave number decreases so fast that the phase no longer increases

$$\theta \to \theta_0 - c_2\omega^3, \tag{15}$$

with constant $c_2(\alpha)$ depending on the details at early times when the long-wave continuum approximation is not applicable.

Substituting our results for the position of the wave packet with frequency, Eqs. (12) and (13), into our expressions for the phase, Eqs. (14) and (15), we find how the phase varies in time and space near to the $k=0$ wave. For $1<\alpha<3$,

$$\theta=\theta_0-\frac{4\sqrt{2}}{3}\left(\frac{3-\alpha}{2\alpha}\right)^{1/2}\left(\frac{z_0(t)-z}{z_0^{1/3}(t)}\right)^{3/2},$$

while for $\alpha>3$,

$$\theta=\theta_0-c_3\left(\frac{z_0(t)-z}{z_0^{(\alpha-1)/2\alpha}(t)}\right)^{3/2},$$

with a constant $c_3(\alpha)$ depending on the early times. From these expressions, we see that at a fixed time the phase changes significantly over a distance

$$L=\begin{cases} z_0^{1/3}(t) & \text{if } 1<\alpha<3 \\ z_0^{(\alpha-1)/2\alpha}(t) & \text{if } \alpha>3, \end{cases}$$

while at a fixed position z, the phase changes significantly in a time

$$T=L/\dot{z}_0.$$

Finally we turn to the variation of the amplitude of the propagating impulse wave. Each component frequency moves with a constant flux of wave action (9), i.e., for the displacements $\tilde{w}(\omega)$,

$$c_g\omega\tilde{w}^2=\text{const}.$$

Thus the maximum displacement decreases according to

$$w_{max}\propto\dot{z}_0^{-1/2}=z_0^{-(\alpha-1)/4\alpha}.$$

The maximum velocity is this typical displacement divided for the time T over which the phase changes significantly, i.e.,

$$v_{max}\propto\begin{cases} z_0^{-(\alpha+3)/12\alpha} & \text{if } 1<\alpha<3 \\ z_0^{-(\alpha-1)/4\alpha} & \text{if } \alpha>3. \end{cases}$$

We plot in Figs. 5 and 6 the exponents β_1 and β_2 obtained numerically and their analytical counterparts. We have a good qualitative agreement between numerical results and analytical prediction as one can see from the crossover at $\alpha=3$ where β_2 begins to increase with the same rate as β_1.

From the above analysis, the displacement and velocity can be written in a self-similar way. If $1<\alpha<3$,

$$\frac{w(z,t)}{z_0^{-(\alpha-1)/4\alpha}(t)}=f_\alpha\left(\frac{z-z_0(t)}{z_0^{1/3}(t)}\right) \quad \text{and}$$

$$\frac{v(z,t)}{z_0^{-(\alpha+3)/12\alpha}(t)}=g_\alpha\left(\frac{z-z_0(t)}{z_0^{1/3}(t)}\right).$$

If $\alpha>3$,

$$\frac{w(z,t)}{z_0^{-(\alpha-1)/4\alpha}(t)}=f'_\alpha\left(\frac{z-z_0(t)}{z_0^{(\alpha-1)/2\alpha}(t)}\right) \quad \text{and}$$

$$\frac{v(z,t)}{z_0^{-(\alpha-1)/4\alpha}(t)}=g'_\alpha\left(\frac{z-z_0(t)}{z_0^{(\alpha-1)/2\alpha}(t)}\right),$$

where f_α, g_α, f'_α, and g'_α are universal functions giving the shape of the pulse. We numerically determined these functions by plotting on the same figure the rescaled pulses at position 1000–9000 with an interval of 1000 between each. Figure 7 displays the results for values of α equal to 1.5, 3.0, and 5.0 confirming a good agreement with the expected scaling behaviors.

V. CONCLUSION

We have studied the problem of the propagation of a weak perturbation in a granular chain subjected to gravity. We first showed numerically that the impulse wave propagating down the vertical column has different features from those observed in a horizontal granular chain. In particular, the amplitude of the waves decrease with depth following power laws. Two power laws for displacement and velocity amplitudes have been found. We proposed a theory that permits us to obtain the functional form of these power-law exponents. Moreover, we found numerically the invariant shape of the displacement and velocity pulses for different values of the force exponent.

The study of the dynamics of the granular column is at its beginning and many other problems remain to be investigated. Concerning the linear regime, one could investigate the case of a perturbation traveling up a column, the symmetry existing for the horizontal chain being broken by gravity. Disorder effects could first be addressed by considering impure columns. The most interesting challenge is perhaps the understanding of the strong anharmonic regime. Although there is a theory for this regime in the case of the horizontal granular chain, this theory does not seem to apply to the granular column.

[1] V.F. Nesterenko, Prikl. Mekh. Tekh. Fiz. **5**, 136 (1983).
[2] V.F. Nesterenko, J. Phys. IV **4**, C8 (1994).
[3] A.N. Lazaridi and V.F. Nesterenko, Prikl. Mekh. Tekh. Fiz. **3**, 115 (1985).
[4] C. Coste, E. Falcon, and S. Fauve, Phys. Rev. E **56**, 6104 (1997).
[5] E.J. Hinch and S. Saint-Jean, Proc. R. Soc. London, Ser. A **455**, 3201 (1999).

[6] E. Hascoët and H.J. Herrmann, Eur. Phys. J. B **14**, 183 (2000).
[7] A. Chatterjee, Phys. Rev. E **59**, 5912 (1999).
[8] E. Hascoët, H. Herrmann, and V. Loreto, Phys. Rev. E **59**, 3202 (1999).
[9] R.S. Sinkovits and S. Sen, Phys. Rev. Lett. **74**, 2686 (1995).
[10] S. Sen and R.S. Sinkovits, Phys. Rev. E **54**, 6857 (1996).
[11] S. Sen, M. Manciu, and J.D. Wright, Phys. Rev. E **57**, 2386 (1998).
[12] J. Hong, J.-Y. Ji, and H. Kim, Phys. Rev. Lett. **82**, 3058 (1999).